IEEE Access
Multidisciplinary ⋮ Rapid Review ⋮ Open Access Journal

Received 5 April 2023, accepted 2 May 2023, date of publication 15 May 2023, date of current version 18 May 2023.

Digital Object Identifier 10.1109/ACCESS.2023.3275962

RESEARCH ARTICLE

Intelligent Motion Control Design for an Omnidirectional Conveyor System

MUHAMMAD QOMARUZ ZAMAN[1] AND HSIU-MING WU[2], (Senior Member, IEEE)
[1]Graduate Institute of Manufacturing Technology, National Taipei University of Technology, Taipei 10608, Taiwan
[2]Department of Intelligent Automation Engineering, National Taipei University of Technology, Taipei 10608, Taiwan

Corresponding author: Hsiu-Ming Wu (hmwu@mail.ntut.edu.tw)

This work was supported by the Taiwan's Ministry of Science and Technology under Grant MOST 111-2221-E-027-130.

ABSTRACT Nowadays, an omnidirectional conveyor system has been introduced as a new means of package transportation. The aim of this study is to achieve trajectory-tracking and collision avoidance of multiple packages which has not been done before on an omnidirectional conveyor platform. Despite the kinematic similarity to omnidirectional mobile robots which have built-in sensors to measure velocities and accelerations, this system only measures the position of the transported package via external sensors which makes it a unique and intriguing area of research. To tackle this challenge, this study employs the proposed Fuzzy Sliding-mode Tracking Control (FSTC) and Fuzzy Inter-package Collision Avoidance (FICA) schemes. The FSTC has been enhanced with fuzzy sliding surfaces that take tracking errors as control inputs and linear forces as control outputs. Furthermore, using a fuzzified package distance and collision angle as inputs, the inference engine of FICA is designed to generate the deflection angle and force gain as outputs. Additionally, the conveyor platform is modeled and built by a multiple modular omnidirectional wheel system including the conveyor and actuator dynamics. To determine its desired motion trajectory, a planned 4th-order Bèzier curve is utilized. Then, to assess the effectiveness and robustness of the proposed methods, simulations are conducted under diverse conditions. The results indicate that the package position converges within a finite time frame, highlighting the superior trajectory-tracking capabilities of FSTC in spite of any disturbances injected into position feedback signals. Meanwhile, the proposed FICA has demonstrated its effectiveness by enabling the package to navigate through the omnidirectional conveyor platform while avoiding both stationary and moving obstacles.

INDEX TERMS Trajectory-tracking, collision avoidance, omnidirectional conveyor, fuzzy sliding-mode tracking control, fuzzy inter-package collision avoidance, 4th-order Bèzier curve.

I. INTRODUCTION

An omnidirectional conveyor system is a type of conveyor system that can move in any direction, including diagonal movements. It is commonly used in the manufacturing and logistics industries for the transportation of goods and materials. The use of omnidirectional conveyor systems has many advantages, including package classification and sorting, flexible route reconfiguration, and improved efficiency in material handling processes [1], [2], [3], [4].

The associate editor coordinating the review of this manuscript and approving it for publication was Kathiravan Srinivasan.

So far, modular design of omnidirectional conveyors has been thoroughly developed in [5], [6], [7], [8], [9], [10], and [11]. Subsequently, a more advanced control such as trajectory-tracking has been made possible. This can be achieved through control of a multiple modular omnidirectional conveyor system. The trajectory control combined with collision avoidance is essential and significant, particularly as a sorting system.

Although the omnidirectional conveyor design is not new, the research on trajectory control in this field is considerably few. Despite the lack of close loop control, some works attempted to put a predefined trajectory on an omnidirectional

conveyor [8], [9], [10], [11]. Later on, a work was done by Sun et al. [12] who developed wheel speed control using PID control. The velocity feedback is done in the actuator level. This way, the entire conveyor platform has predefined velocity and direction. On the other hand, works in [13] and [14] used a different PID control approach that allowed an individual conveyor module to change velocity and correct the package position. Also, there is conducted research for an omnidirectional conveyor using reinforcement learning [15]. However, the proposed method did not produce continuous control inputs. The common challenge based on the previous works is it is hard to acquire the dynamic model of the platform. The dynamics form dictates the way control schemes used.

A single omnidirectional conveyor module shares kinematic similarities with omni-wheeled mobile robots. Trajectory-tracking research has been conducted on these robots, utilizing state-space control techniques (Refs. [16], [17], [18]) and sliding-mode control techniques (Refs. [19], [20], [21]). However, these approaches required numerous sensors including velocity, acceleration, torque, or current sensors to be installed in the robot for successful implementation. Referring to Refs. [1], [2], and [14], it can be observed that dissimilar to the prior approaches, the transported packages are not equipped with sensors. Instead, an omnidirectional conveyor system typically employs a camera or proximity sensor to externally determine the position of the package. Furthermore, the aforementioned model-based control techniques are optimized specifically for omni-wheeled mobile robots and may not be directly compatible with an omnidirectional conveyor system. Thus, further investigation is necessary to develop effective trajectory-tracking solutions for omnidirectional conveyor systems.

Further, there is little research on inter-package collision avoidance of omnidirectional conveyor systems. Despite the difference in terms of dynamics, some previous works addressing this matter are available in the field of mobile robots; for example, a study in [22] developed a complex if-then rules and the works in [23], [24], [25], and [26] developed fuzzy inference systems to avoid obstacles. The common issue (based on these previous works) is to design a smooth transition between the trajectory tracking and obstacles avoidance control.

This study proposes an intelligent control scheme with high-level robustness, i.e., Fuzzy Sliding-mode Tracking Control (FSTC) and Fuzzy Inter-package Collision Avoidance (FICA) techniques, to make a package track the desired trajectory on an omnidirectional conveyor and avoid possible collision between packages. The contributions are enumerated as follows:

1) A dynamic model is developed for an omnidirectional conveyor system. The omnidirectional platform is based on Refs. [12] and [13], however, the dynamic and actuator models in the research are introduced as they have not been studied in Refs. [12], [13], [14], abd [15]. Without the dynamic model, the control inputs become discretized as presented in Ref. [15].
2) A close-loop control with package position feedback is completely executed. A different control approach is used compared to the PID used in Refs. [12], [13], and [14]; FSTC is utilized in this research since it is more robust in the area of non-linear controllers. In addition, the control input for the entire conveyor platform is not predefined. Instead, each individual module has a dynamic velocity and direction contrasting with Refs. [8], [9], [10], [11], [12], and [15]. Furthermore, dissimilar to Refs. [8], [9], [10], [11], [12], [15], [16], [17], [18], [19], [20], and [21], the trajectory tracking is achieved by using a feedback from the position of the package and the control inputs are actuated on each conveyor module independently via actuator voltages.
3) A mission for collision avoidance between packages is successfully achieved. The FICA technique has the advantage of fuzzy interpolative reasoning unlike the hard computing technique utilized by Ref. [22]. This also includes a seamless switching between trajectory tracking and obstacle avoidance by fuzzy inference engine contrasting with Refs. [23] and [25]. The inference engine has numerous simplicity in comparison with Refs. [23], [24], [25], and [26] leading to a reduction of computation power demands. Combined with FSTC, FICA makes a multiple intersecting trajectories tracking possible, dissimilar to predefined trajectories in works [8], [9], [10], [11], [12], [15].

The remaining sections of the paper are organized as follows: In Section II, the system modelling of the multiple modular omnidirectional conveyor module is described and the problem statement is presented. In Section III, the design of the proposed FSTC is explained. In addition, section IV describes the FICA design for collision avoidance. The simulation results and discussions are presented in Section V. Finally, concluding statements are given in Section VI.

II. SYSTEM MODELING AND PROBLEM FORMULATION

An omnidirectional conveyor system is typically used to overcome two overlapping conveyor belts from different directions. It can direct the flow on a conventional conveyor from one end to another. Also, it is used as a sorting bed before transferring goods from one conveyor belt to another as shown in Fig. 1. In both situations, the package must follow a prescribed trajectory. The omni-wheels on the conveyor are utilized to control the moving position of the packages according to the planned trajectory. Hence, a dynamic model of the system must be derived to

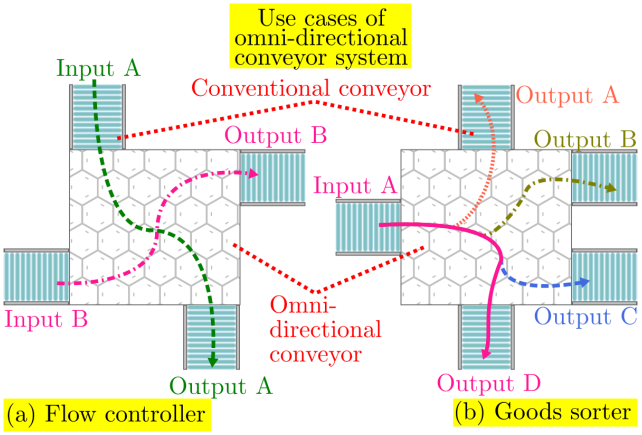

FIGURE 1. The use cases of omnidirectional conveyor system together with conventional conveyor system.

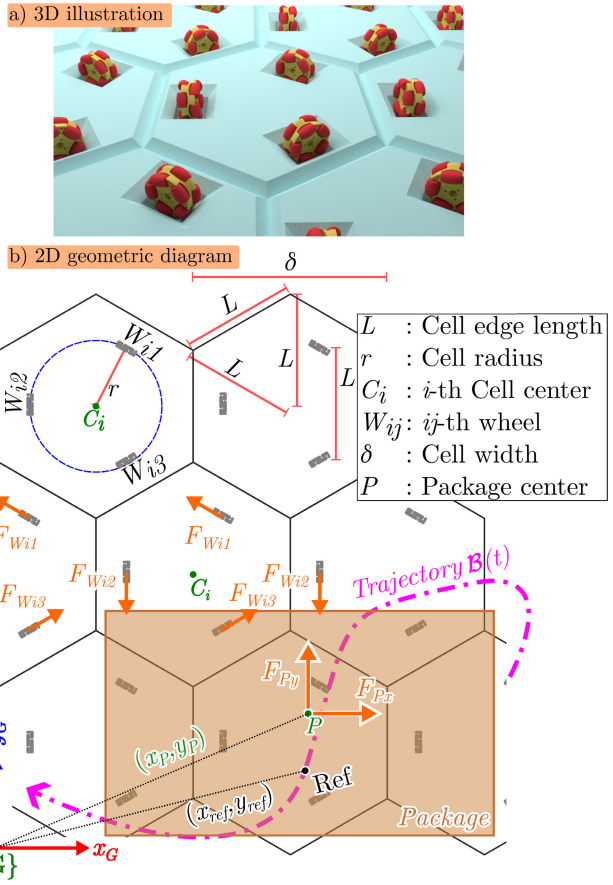

FIGURE 2. The illustration of an omnidirectional conveyor system.

enable the velocity transferred from each omni-wheel to the package.

The conveyor system is driven by DC motors equipped with omni-wheels. A single module is designed as a hexagonal shape with three omni-wheels as shown in Fig. 2. In a polar coordinates relative to the ith module frame $\{C_i\}$, the omni-wheels positions $W_{ij}(r_j, \theta_j)$ are at $\{(r, \frac{\pi}{3}), (r, \pi), (r, -\frac{\pi}{3})\}$ where i is the index of modules and $j \in \{1, 2, 3\}$ is the index of the omni-wheels. Together with the hexagonal chassis, there exist some properties in the module i.e. the length of the hexagonal edge is $L = \sqrt{3}r$ and the width of the module is $\delta = 3r$.

The force direction and magnitude of the package on the conveyor are determined by the force resultant of omni-wheels laying underneath the package. From the geometric relationship shown in Fig. 2, a package dynamics is given by

$$\begin{aligned} m\ddot{x}_P &= F_{Px} - \mu\dot{x}_P \\ m\ddot{y}_P &= F_{Py} - \mu\dot{y}_P \end{aligned} \tag{1}$$

where

$$\begin{bmatrix} F_{Px} \\ F_{Py} \end{bmatrix} = \begin{bmatrix} -\frac{\sqrt{3}}{2} & 0 & \frac{\sqrt{3}}{2} \\ \frac{1}{2} & -1 & \frac{1}{2} \end{bmatrix} \begin{bmatrix} \sum^{k} F_{Wk1} \\ \sum^{k} F_{Wk2} \\ \sum^{k} F_{Wk3} \end{bmatrix} \tag{2}$$

where F_{Px} and F_{Py} are respectively the forces of the package along X and Y-axes; μ is a viscous friction constant of the package; m is the mass of the package. Here, $k \subset i$ represents module index number under the package and $F_{Wk1,2,3}$ are the corresponding omni-wheels touching the bottom of the package. To infer this law, the package is assumed to be bigger than $2\delta \times \delta$ m^2 to ensure that there is a package transfer between 2 neighboring modules. By considering the inertia I_W, viscous friction constant ζ, angular velocity ω_W, and radius r_W of the wheel, the dynamics of each wheel is defined as

$$I_W\dot{\omega}_{Wij} + \zeta\omega_{Wij} = \tau_{Wij} - r_W F_{Wij} \tag{3}$$

where τ_{Wij} denotes generated torques from omni-wheels. Here, the omni-wheels are actuated by DC motors in which mathematical model is given as

$$\begin{cases} V_{Wij} = R_a i_a + L_a \dfrac{di_a}{dt} + e_a \\ e_a = K_b \omega_{Wij} \\ \tau_{Wij} = K_t i_a \end{cases} \tag{4}$$

where V_{Wij} is the input voltage of ijth the motor; R_a, i_a, L_a, and e_a are respectively armature resistance, current, inductance, and back emf voltage; K_b and K_t are respectively back emf and torque constants.

The objective of the study is to transfer a package across an omnidirectional conveyor system from one end to the other. To achieve this goal, we propose the FSTC technology that tracks the package's movement along a prescribed trajectory. The tracking error between the actual position and intended trajectory is computed and then used in constructing sliding surfaces. A fuzzy inference engine analyzes these sliding surfaces to determine actuation voltage for the omni-wheels, aiming to adjust tracking errors towards zero. A detailed description about the calculation of tracking errors and sliding surfaces can be found in the subsequent section of this paper.

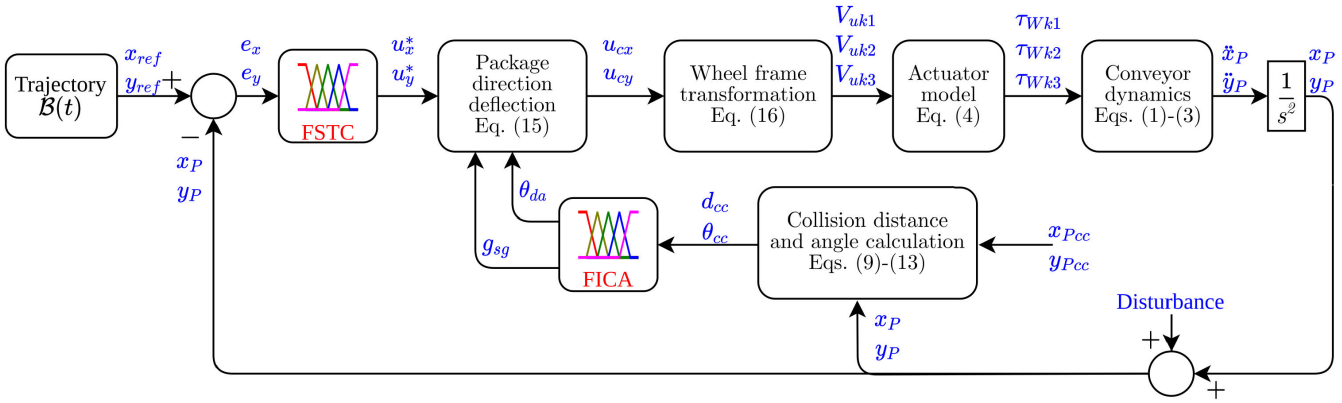

FIGURE 3. Overall control block diagram.

Moreover, the FICA approach is proposed to prevent collisions between multiple packages on the omnidirectional conveyor system. For this purpose, it is essential to maintain a distance greater than zero between package boundaries. The proposed FICA infers the distance between colliding packages and the direction of trajectory tracking in order to produce magnitude and direction of the avoidance. The overall control scheme is shown in Fig. 3. Further mathematical descriptions of the proposed controller will be provided in the subsequent section.

III. FUZZY SLIDING-MODE TRACKING CONTROL DESIGN

At first, through the planned motion trajectory function $\mathcal{B}(t)$, a new reference pose (x_{ref}, y_{ref}) is fed to the controller for the following of the package as t evolves. Then, by using the integration of the dynamic Eqs. (2) and (4), the position of the package (x_P, y_P) with respect to the global coordinate can be obtained. In this way, tracking errors e_x and e_y can be calculated as follows:

$$\begin{bmatrix} e_x \\ e_y \end{bmatrix} = \begin{bmatrix} x_{ref} \\ y_{ref} \end{bmatrix} - \begin{bmatrix} x_P \\ y_P \end{bmatrix} \tag{5}$$

It is well-known that the robust controller, FSTC, can deal with the uncertain control systems very well. To begin with, sliding surfaces are designed based on the error information as shown in the following Eq. (6)

$$\begin{cases} \sigma_x = a_x e_x + b_x \dot{e}_x \\ \sigma_y = a_y e_y + b_y \dot{e}_y \end{cases} \tag{6}$$

where the chosen constants $a_{x,y}, b_{x,y} > 0$ such that the sliding surfaces are stable. Then, the sliding surfaces as inputs are fuzzified and the input fuzzy membership functions $(\mu_{\sigma x}, \mu_{\sigma y})$ are designed in Fig. 4a. Here, $\{NL, NM, NS, Z, PS, PM, PL\}$ are the linguistic representations of Negative Large, Negative Medium, Negative Small, Zero, Positive Small, Positive Medium, and Positive Large respectively. The outputs of the fuzzy system are the control commands proportional to the forces of the package (u_x, u_y) in the global coordinate. The inputs σ_x and σ_y can

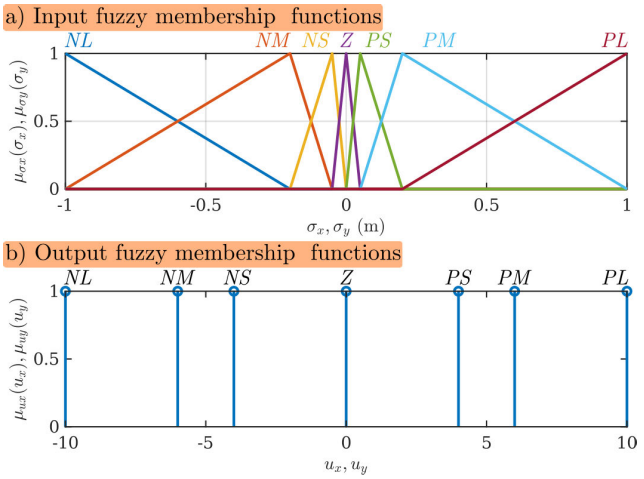

FIGURE 4. Input and output fuzzy membership functions.

be normalized by gain values if needed. That is to say, the membership value ranges of the $\mu_{\sigma x}$ and $\mu_{\sigma y}$ are between $[-1, 1]$. This also applies to the membership value ranges of μ_{ux} and μ_{uy} which are estimated voltage outputs of the package that can be adjusted by gains. The designed output fuzzy membership functions (μ_{ux}, μ_{uy}) are singleton type as shown in Fig. 4b that is proven for effective elimination of chattering effects [27].

Incorporating an expert's knowledge is the common approach to design fuzzy membership functions. However, a significant number of fuzzy membership functions result in more intricate computation and inference rules. Furthermore, as each package has its own FSTC, the computational load also increases with the number of packages. To simplify computation, this study selects only seven membership functions for FSTC scheme. Here, the most important memberships for the FSTC are Z, PL, and NL. The purpose of the Z membership function is to produce a fuzzy output value of 0 when the tracking error falls between ± 0.05 m. For tracking errors exceeding ± 1 m, fuzzy outputs are handled by both PL and NL with corresponding values

of ± 10. Besides, *NM*, *NS*, *PM*, and *PS* fuzzy membership functions are introduced to ensure smoother transitions between *Z*, *PL*, and *NL* and prevent overshoots in the tracking response.

Next, fuzzy inference rules are designed such that the designed sliding surfaces $\sigma_x \to 0$ and $\sigma_x \to 0$ are achieved as $t \to \infty$. Subsequently, the tracking errors asymptotically converge to zero. To do so, the input fuzzy membership functions are paired with the output fuzzy membership functions accordingly to form inference rules as (7):

$$\begin{array}{lll} \mathfrak{R}_1 & : if(\sigma_i = NS) & then(u_i = NS) \\ \mathfrak{R}_2 & : if(\sigma_i = NM) & then(u_i = NM) \\ \vdots & \vdots & \vdots \\ \mathfrak{R}_7 & : if(\sigma_i = PL) & then(u_i = PL) \end{array} \tag{7}$$

The consequence functions $(\hat{\mu}_{ux}, \hat{\mu}_{uy})$ of the rules are defuzified using the center of gravity approach as

$$\begin{cases} u_x^* = \dfrac{\sum\limits_{u_x} u_x \, \hat{\mu}_{ux}(u_x)}{\sum\limits_{u_x} \hat{\mu}_{ux}(u_x)} \\ u_y^* = \dfrac{\sum\limits_{u_y} u_y \, \hat{\mu}_{uy}(u_y)}{\sum\limits_{u_y} \hat{\mu}_{uy}(u_y)} \end{cases} \tag{8}$$

The next section will focus on the approach of collision avoidance of multiple moving packages.

IV. FUZZY INTER-PACKAGE COLLISION AVOIDANCE DESIGN

As two packages (P and P_{cc}) simultaneously move on the conveyor system, one package needs to avoid another package in case another package is on the trajectory at the same time. Here, a fuzzy inference control technique, i.e. FICA, is proposed to attain the task. Fig. 5 illustrates the geometric relations for the package positions in the global frame $\{G\}$. In this section, the proposed FICA is applied only to a package P to avoid package P_{cc}. The same FICA technique can be applied to another package. In this case, two moving packages are expected to avoid each other when the FICA techniques are applied to both packages.

The proposed FSTC and FICA are applied to make the package $P(x_P, y_P)$ track the trajectory $\mathcal{B}(t)$ and avoid the package $P_{cc}(x_{Pcc}, y_{Pcc})$. Here, (x_{ref}, y_{ref}) is a reference point on the planned trajectory $\mathcal{B}(t)$. In a polar coordinate relative to a point P, the Euclidean distance d_{pp} from P to P_{cc} is given by

$$d_{pp} = \sqrt{(x_{Pcc} - x_P)^2 + (y_{Pcc} - y_P)^2} \tag{9}$$

and the polar angle θ_{cx} is given by

$$\theta_{cx} = \text{atan2}((y_{Pcc} - y_P), (x_{Pcc} - x_P)) \tag{10}$$

where atan2(·) is an inverse tangent function that returns values in $[-\pi, \pi]$ [28], [29], [30], [31]. By using the similar

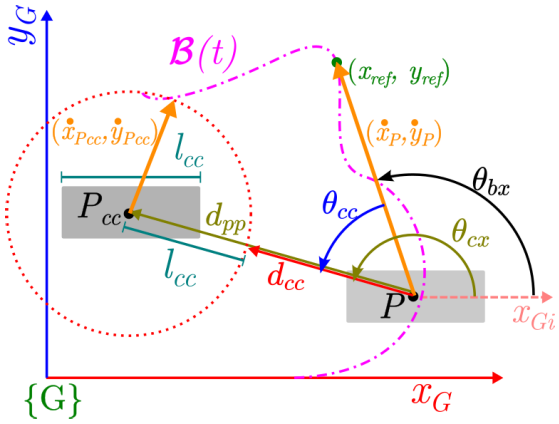

FIGURE 5. Packages position relation diagram.

TABLE 1. Listed fuzzy rules for obstacle avoidance.

Z_{sg} / Z_{da}		$X_{\theta c}$			
		BN	N	P	BP
X_{dc}	N	0.05 $\pi + \theta_{cc}$	0.05 $\pi + \theta_{cc}$	0.05 $\theta_{cc} - \pi$	0.05 $\theta_{cc} - \pi$
	M	1 0	0.2 $\frac{\pi}{2} + \theta_{cc}$	0.2 $\frac{\pi}{2} + \theta_{cc}$	1 0
	F	1 0	1 0	1 0	1 0

principle, the polar angle of a reference point θ_{bx} is calculated as follows:

$$\theta_{bx} = \text{atan2}((y_{ref} - y_P), (x_{ref} - x_P)) \tag{11}$$

Using (10) and (11), a collision candidate angle θ_{cc} can be obtained by

$$\begin{cases} \hat{\theta}_{cc} = \theta_{cx} - \theta_{bx} \\ \theta_{cc} = \text{atan2}(\sin(\hat{\theta}_{cc}), \cos(\hat{\theta}_{cc})) \end{cases} \tag{12}$$

Here, the value θ_{cc} is normalized between $[-\pi, \pi]$ using atan2(·) function. Then, the collision candidate distance d_{cc} can be obtained by

$$d_{cc} = d_{pp} - l_{cc} \tag{13}$$

where l_{cc} is a preferred safe distance between packages. In this study, l_{cc} is chosen to be equal to the width of package P_{cc}.

The collision avoidance goal can be achieved by inferring from d_{cc} and θ_{cc}. Fuzzy membership functions $(\mu_{dc}, \mu_{\theta c})$ are designed to respectively represent the d_{cc} and θ_{cc} in linguistic terms of $X_{dc} = \{N : \text{Near}, M : \text{Medium}, F : \text{Far}\}$ and $X_{\theta c} = \{BN : \text{Big Negative}, N : \text{Negative}, P : \text{Positive}, BP : \text{Big Positive}\}$. The triangular membership functions $\mu_{dc}(d_{cc})$ and $\mu_{\theta c}(\theta_{cc})$ are depicted in the Fig. 6. The collision avoidance inference engine is to use two inputs $(X_{dc}, X_{\theta c})$ and generate two outputs (Z_{sg}, Z_{da}) with the following fuzzy rules listed in Table 1.

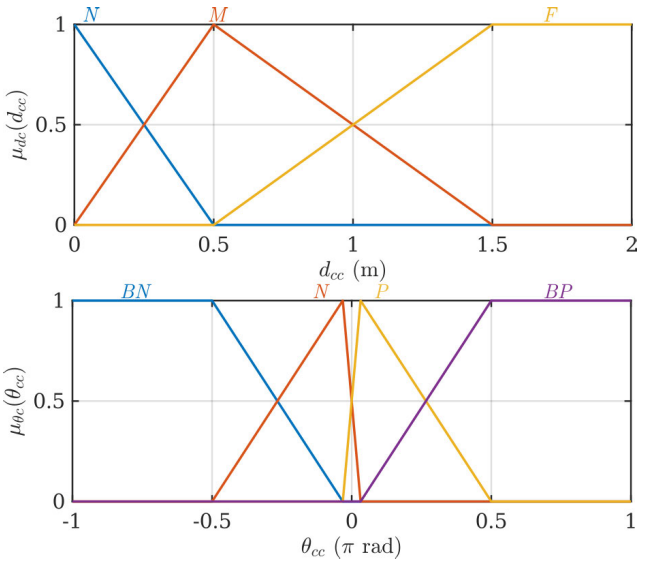

FIGURE 6. Membership functions of $\mu_{dc}(d_{cc})$ and $\mu_{\theta c}(\theta_{cc})$.

The accumulated outputs of the fired rules are defuzzified using the weighted average approach as follows:

$$\begin{cases} g_{sg} = \dfrac{\sum\limits_R \mu_R Z_{sgR}}{\sum\limits_R \mu_R} \\ \theta_{da} = \dfrac{\sum\limits_R \mu_R Z_{daR}}{\sum\limits_R \mu_R} \end{cases} \tag{14}$$

where μ_R denotes the firing degree of rule R and (Z_{daR}, Z_{sgR}) are singleton output values of a gain (g_{sg}) and deflection angle (θ_{da}) of rule R. To avoid collision while there is a package close by, the proposed FICA technique adjusts the magnitude and direction of the outputs (u_x^*, u_y^*) generated from the proposed FSTC by the factor g_{sg} and θ_{da} respectively as

$$\begin{bmatrix} u_{cx} \\ u_{cy} \end{bmatrix} = g_{sg} \begin{bmatrix} \cos\theta_{da} & -\sin\theta_{da} \\ \sin\theta_{da} & \cos\theta_{da} \end{bmatrix} \begin{bmatrix} u_x^* \\ u_y^* \end{bmatrix} \tag{15}$$

Because the control inputs are represented in the global frame $\{G\}$, a transformation to the wheel frame $\{W_{ij}\}$ is needed. Hence, using the geometric relationship shown in Fig. 2, the following equation can be obtained as

$$\begin{bmatrix} V_{uk1} \\ V_{uk2} \\ V_{uk3} \end{bmatrix}_{k\subset i} = \begin{bmatrix} -\frac{\sqrt{3}}{2} & \frac{1}{2} \\ 0 & -1 \\ \frac{\sqrt{3}}{2} & \frac{1}{2} \end{bmatrix} \begin{bmatrix} u_{cx} \\ u_{cy} \end{bmatrix} \tag{16}$$

where $V_{uk1,2,3}$ are input voltages for the actuators under the package.

V. SIMULATION RESULTS AND DISCUSSIONS

To investigate the feasibility of the proposed control schemes, the trajectory-tracking and collision avoidance of a multiple modular omnidirectional conveyor system is simulated with the parameters listed in Table 2.

TABLE 2. Simulation parameters.

Parameter	Value
r	12 cm
R_a	1 mΩ
L_a	1 mH
K_b	4.5×10^{-2} V/rad/s
K_t	7×10^{-2} N/A
r_W	3 cm
I_W	4.5×10^{-5} kgm^2
m	2 kg
μ	98 N/m/s
ζ	0.3 N/rad/s
$a_{x,y}$	3
$b_{x,y}$	0.2

As illustrated by the use cases of the omnidirectional conveyor system in Fig. 1, the purpose of the omnidirectional conveyor system is to transfer a package from one end to the other. Unlike circular or lemniscate trajectories that form a loop, an open-end trajectory that connects two points is used for this task. Moreover, a trajectory may appear in various shapes in real applications. Therefore, the package is simulated to follow a trajectory generated from a Bézier curve in this study. A Bézier curve is one of the most intuitive parametric functions that can form any shape and has been widely used in computer-aided design software.

A $4th$-order Bézier curve trajectory $\mathcal{B}_1(s)$; $s \in [0, 1]$

$$\mathcal{B}_1(s) = \begin{bmatrix} s^0 & s^1 & \dots & s^4 \end{bmatrix} \cdot \begin{bmatrix} 1 & 0 & 0 & 0 & 0 \\ -4 & 4 & 0 & 0 & 0 \\ 6 & -12 & 6 & 0 & 0 \\ -4 & 12 & -12 & 4 & 0 \\ 1 & -4 & 6 & -4 & 1 \end{bmatrix} \begin{bmatrix} 1 & 1 \\ \frac{21}{4} & \frac{1}{3} \\ \frac{11}{2} & 5 \\ \frac{23}{4} & \frac{29}{3} \\ 10 & 9 \end{bmatrix} \tag{17}$$

is planned as a motion trajectory of moving packages.

The conveyor is arranged to move on an 10×10 m^2 floor. The prescribed trajectory starts at $(1, 1)$ and ends at $(10, 9)$ giving out approximately 13.38 m of the path length. Two initial cases are performed independently in sequential order, namely case #1 and case #2 which have the initial positions of $(0, 4)$ and $(4, 0)$, respectively. Both packages must be transferred from one end to the other one within 20 s i.e. $s = \frac{t}{20}$.

First, under the given prescribed trajectory and initial conditions, a PID control method is applied as a baseline performance whose results are shown in Fig. 7. It can be seen that a bit of tracking error arises and further details are shown in Fig. 8. The results demonstrate that the package converges to the prescribed trajectory within 1.5 s with a maximum error of 0.32 m.

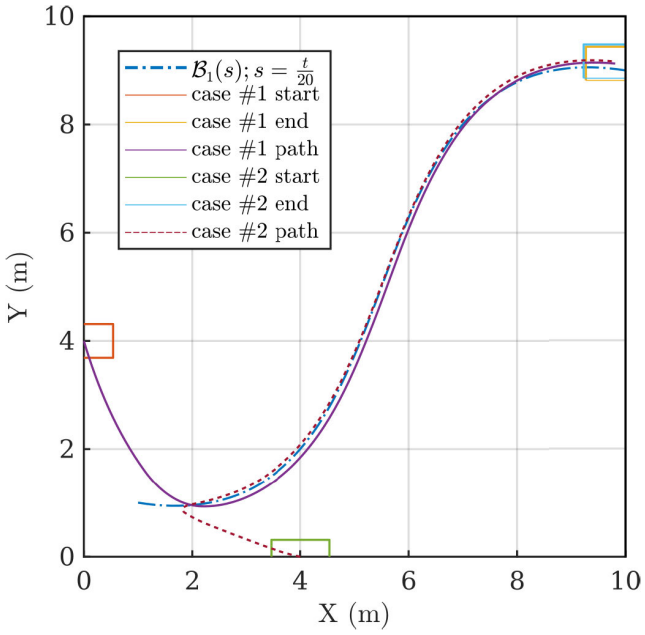

FIGURE 7. Package movement along the prescribed trajectory using PID.

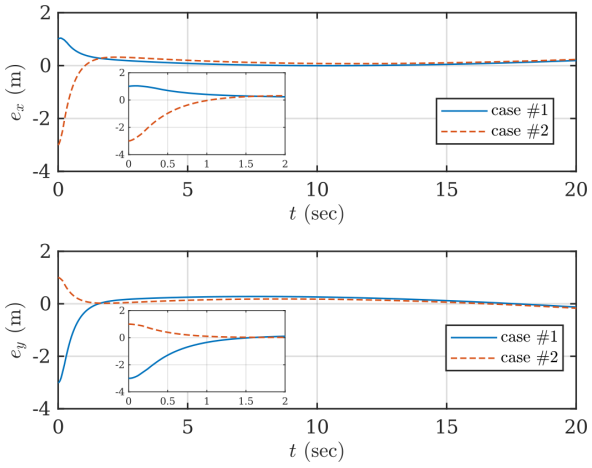

FIGURE 8. Responses of e_x and e_y with time history using PID for cases #1 and #2.

Second, FSTC is applied under the same trajectory and initial conditions. The tracking response is shown in Fig. 9 where tracking errors are smaller compared to results of the PID method. The trajectory-tracking accuracy can be seen clearly in the error response shown in Fig. 10. As observed from the figure, the tracking responses are quite satisfactory. Furthermore, the proposed FSTC has a fast response as the errors approach to zero within 1 s. Aligned with the error response, the sliding surfaces also converge to zero within 1 s as shown in Fig. 11. The corresponding voltages generated by the FSTC are demonstrated in Fig. 12. From the figure, the chattering phenomenon is indeed reduced by means of the designed fuzzy singleton-type outputs. As stated in Ref. [27], fuzzy membership functions can improve the control system's performance to handle disturbances and uncertainties.

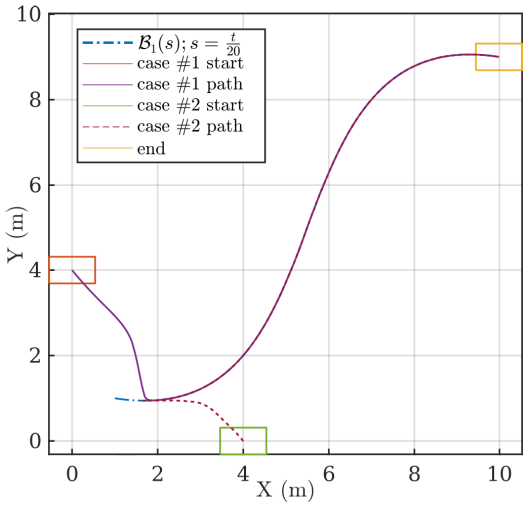

FIGURE 9. Package movement along the prescribed trajectory using FSTC.

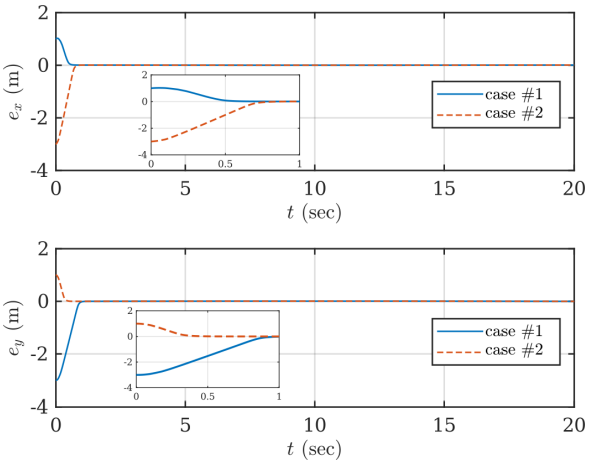

FIGURE 10. Responses of e_x and e_y with time history using FSTC for cases #1 and #2.

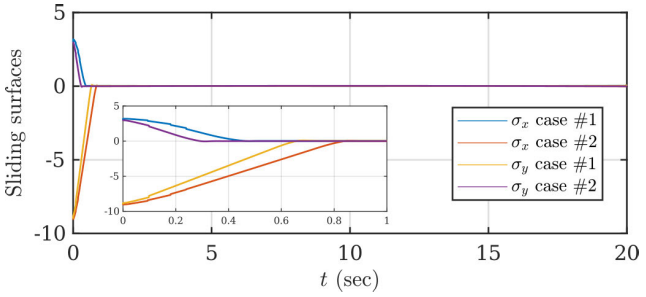

FIGURE 11. Responses of σ_x and σ_y with time history for cases #1 and #2.

When utilizing fuzzy logic control, alterations to a crisp value may not necessarily impact the corresponding linguistic term. This results in the reduction of the chattering effect on the control output.

Third, to investigate the feasibility of the proposed FICA, a static package is placed at $(6, 4)$ in which the moving

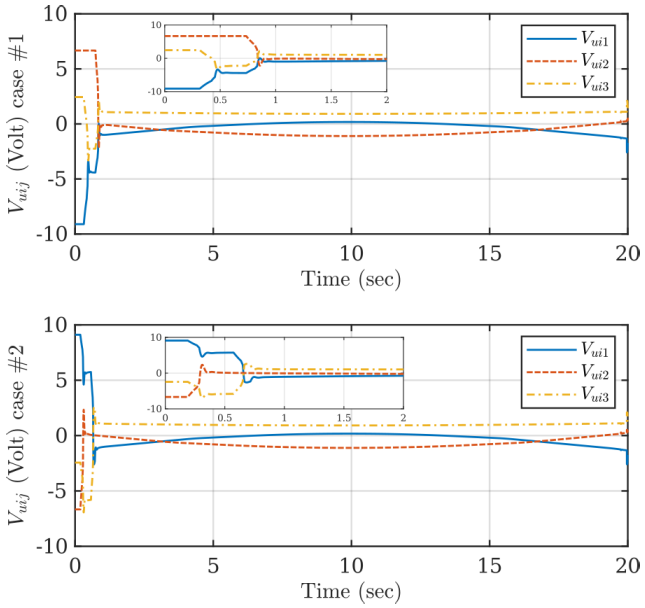

FIGURE 12. Responses of V_{uij} with time history using FSTC for cases #1 and #2.

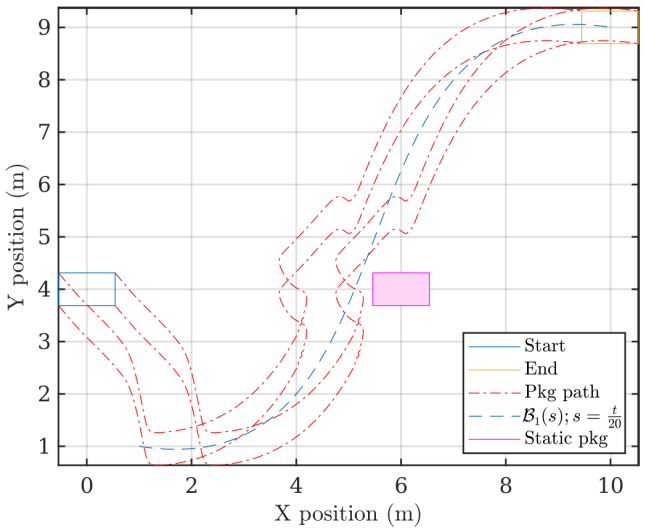

FIGURE 13. The movement of the moving package on the prescribed trajectory while avoiding a static package on its path.

package would collide and the moving package is initially placed at $(4, 0)$. The response is shown in Fig. 13 where the red dash-dotted lines represent the movement trajectory of the package corners. We can see that collision of the moving package does not happen with the static package. In addition, the responses of g_{sg} and θ_{da} for the moving package are exhibited in Fig 14. It is observed that the moving package turns left corresponding to the positive value of θ_{da}.

Fourth, to examine the performance of the proposed FSTC and FICA, an additional intersecting trajectory is designed as

$$\mathcal{B}_2(s) = \begin{bmatrix} s^0 & s^1 & \dots & s^4 \end{bmatrix}$$

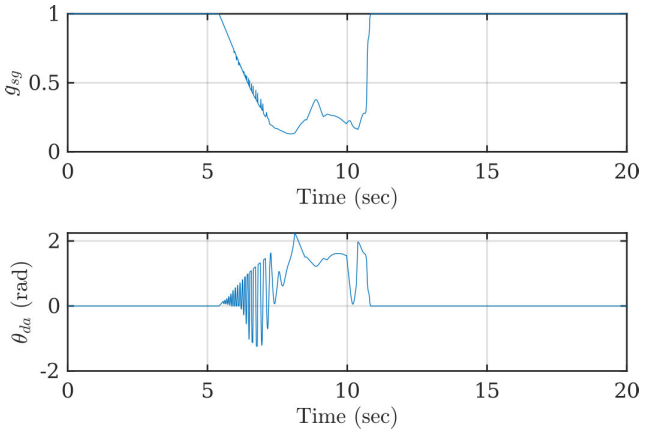

FIGURE 14. Responses of g_{sg} and θ_{da} for the moving package.

$$\cdot \begin{bmatrix} 1 & 0 & 0 & 0 & 0 \\ -4 & 4 & 0 & 0 & 0 \\ 6 & -12 & 6 & 0 & 0 \\ -4 & 12 & -12 & 4 & 0 \\ 1 & -4 & 6 & -4 & 1 \end{bmatrix} \begin{bmatrix} 9 & 1 \\ \frac{15}{2} & 4 \\ 5 & 5 \\ \frac{5}{2} & 6 \\ 1 & 10 \end{bmatrix} \tag{18}$$

for a second moving package. The packages are initially located at $\{(0, 4), (7, 0)\}$ respectively for the first and the second packages. The proposed FSTC and FICA are applied to both of the moving packages. The movement history of both packages is shown in Fig. 15. It can be seen that the second package avoids the first package by turning northward at $t = 9$ and then followed by the turning of the first package eastward at $t = 10$. This shows that both packages can avoid collision with each other. Moreover, between $t = 9$ and $t = 13$, both packages successfully avoid each other without collision and then return to the individual prescribed trajectories once the path is clear from a possible collision.

Fifth, a Gaussian noise is injected into the position feedback signals of the packages (see Fig. 3) to examine the robustness of the proposed control schemes. Usually, the position feedback signals of the packages are contaminated, either caused by uncertainties in the dynamics, such as friction, or some noises in the measurement. For these reasons, to show the robustness of the proposed FSTC and FICA, a Gaussian noise with the mean of 0 m and variance of 0.1 m is added to the position feedback of the two packages. The initial conditions and planned trajectories of the packages are the same with the fourth simulation. The result is demonstrated in Fig. 16. As observed from the movement history, both packages successfully avoid each other and both packages converge to the individual prescribed trajectories between $12 < t < 20$ s. Thus, the trajectory tracking and collision avoidance performances are satisfactory even under disturbances injected into position feedback signals.

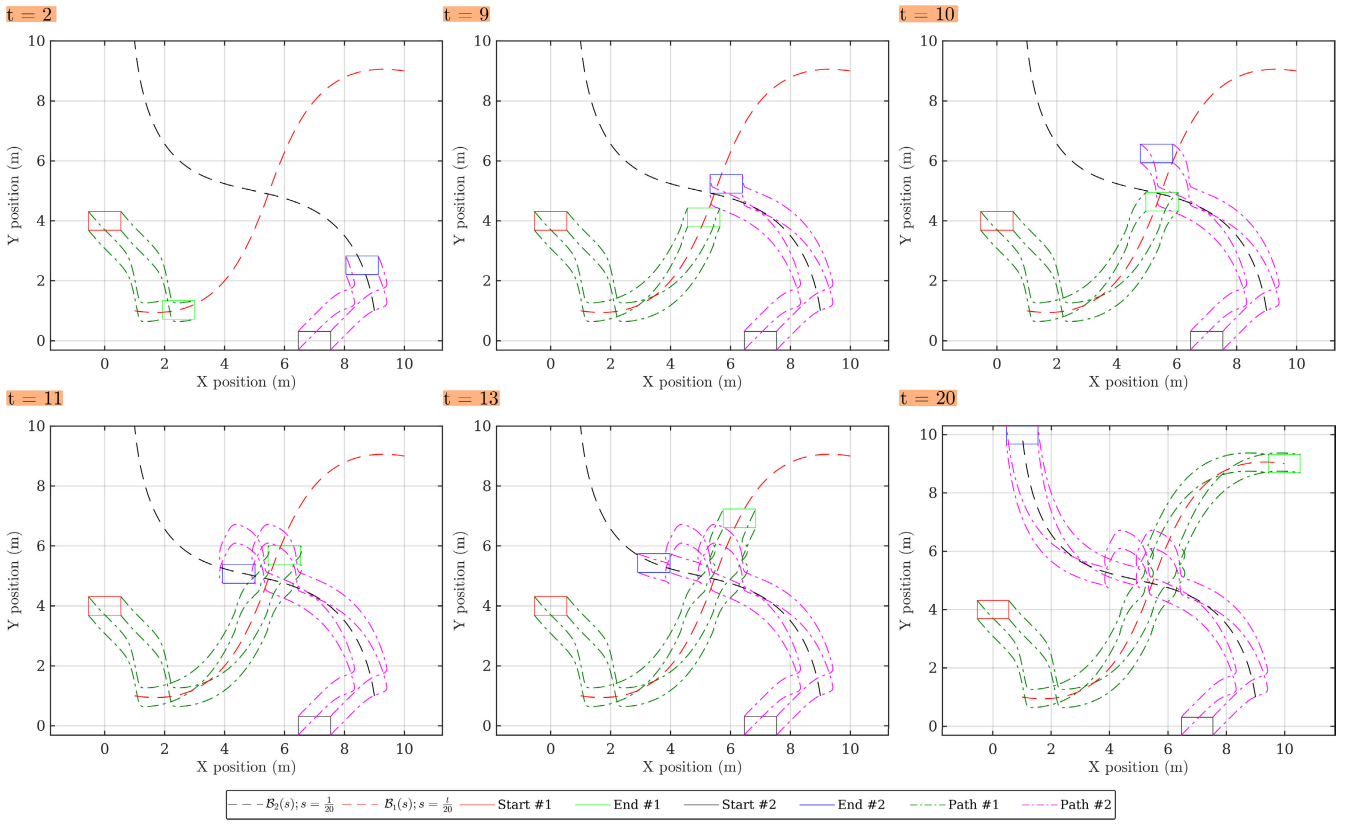

FIGURE 15. Movement history of the first package following $\mathcal{B}_1(s)$ trajectory and the second package following $\mathcal{B}_2(s)$ trajectory while avoiding collision from each other.

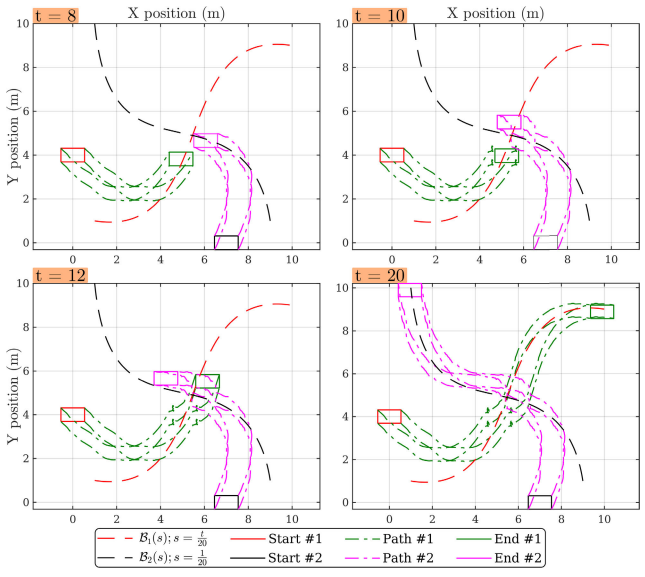

FIGURE 16. Movement history of the first package following $\mathcal{B}_1(s)$ trajectory and the second package following $\mathcal{B}_2(s)$ trajectory while avoiding collision from each other with Gaussian noise added to the packages positions feedback.

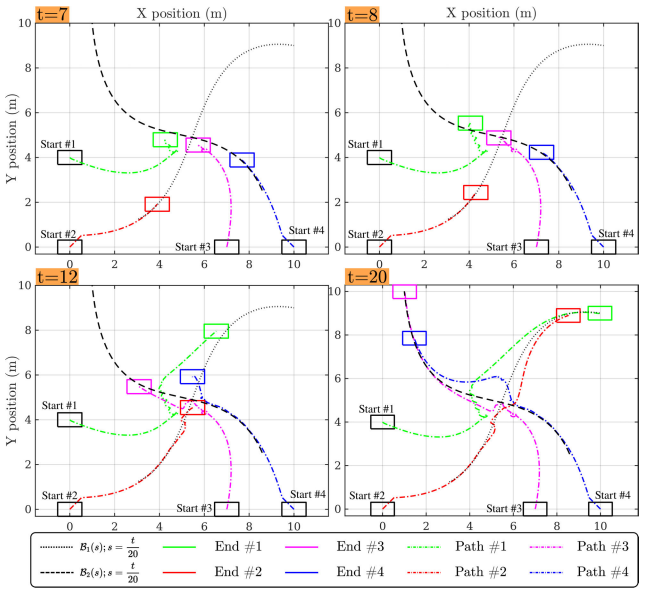

FIGURE 17. The movement history of four packages, two following the trajectory $\mathcal{B}_1(s)$ and two following the trajectory $\mathcal{B}_2(s)$, without colliding with each other.

Sixth, four packages are placed at the same time on the omnidirectional conveyor system. Their initial positions, as displayed in Fig. 17, are {(0, 4), (0, 0), (7, 0), (10, 0)}. It is worth noting that a practical scenario could involve collision risks between the front and back of packages. To demonstrate

how FSTC and FICA handle this situation effectively, one trajectory is set to be used by two packages. At $t = 7$ s in the simulation, all the packages approach the trajectories to bring about a possible collision event between the first and third packages. By passing through the front of the third package at $t = 8$ s, the first package is able to resolve the situation. Simultaneously, while sensing a potential collision between its front and back, the third package efficiently maintains its distance to prevent any collision. The first package then proceeds to cross over successfully and return to its dedicated trajectory by $t = 12$. At this same time point, in order to steer clear from each other, both the fourth and second packages adjusted their positions accordingly. Finally, all packages successfully avoid each other by $t = 20$ and safely return to their respective planned trajectories.

VI. CONCLUSION

In this study, the FSTC technique is proposed to track the planned trajectory for a package on an omnidirectional conveyor platform. The motion trajectory is planned using the 4th-order Bézier curve. Two cases in different initial positions are investigated under the proposed FSTC. Moreover, the FICA approach is presented to achieve collision avoidance of multiple moving packages. Furthermore, two intersecting trajectories for two packages are designed to investigate the feasibility and robustness of the proposed FSTC and FICA under disturbances injected into position feedback signals. The simulation results validate the effectiveness and feasibility of the proposed control schemes.

In our future work, we aim to develop a vision-based system to recognize package size and position. This will involve implementing an object detection algorithm that has been enhanced through a deep learning technology. Furthermore, proximity sensors will be placed on each wheel to assist with package recognition. Additionally, the proximity sensor will aid in reducing energy consumption by deactivating the wheel that is not in contact with the package. This research direction will make the implementation of the proposed FSTC and FICA more feasible in real-world scenarios.

REFERENCES

[1] E. B. Salazar, B. N. Escudero, and S. N. R. Minango, "Omnidirectional transport system for classification and quality control using artificial vision," in *Proc. 3rd Int. Conf. Virtual Augmented Reality Simulations*, Feb. 2019, pp. 62–66.

[2] M. E. El-Sayed, A. W. Youssef, O. M. Shehata, L. A. Shihata, and E. Azab, "Computer vision for package tracking on omnidirectional wheeled conveyor: Case study," *Eng. Appl. Artif. Intell.*, vol. 116, Nov. 2022, Art. no. 105438.

[3] M. B. Firvida, H. Thamer, C. Uriarte, and M. Freitag, "Decentralized omnidirectional route planning and reservation for highly flexible material flow systems with small-scaled conveyor modules," in *Proc. IEEE 23rd Int. Conf. Emerg. Technol. Factory Autom. (ETFA)*, vol. 1, Sep. 2018, pp. 685–692.

[4] A. W. Youssef, N. M. Elhusseiny, O. M. Shehata, L. A. Shihata, and E. Azab, "Kinematic modeling and control of omnidirectional wheeled cellular conveyor," *Mechatronics*, vol. 87, Nov. 2022, Art. no. 102896.

[5] S. H. Mayer, "Development of a completely decentralized control system for modular continuous conveyors," Ph.D. dissertation, Karlsruher Institut für Technol. (KIT), Karlsruhe, Germany, 2009.

[6] L. Overmeyer, K. Ventz, S. Falkenberg, and T. Kruhn, "Interfaced multi-directional small-scaled modules for intralogistics operations," *Logistics Res.*, vol. 2, nos. 3–4, pp. 123–133, Dec. 2010.

[7] C.-N. Wang, Y.-H. Wang, H.-P. Hsu, and T.-T. Trinh, "Using rotacaster in the heuristic preemptive dispatching method for conveyor-based material handling of 450 mm wafer fabrication," *IEEE Trans. Semicond. Manuf.*, vol. 29, no. 3, pp. 230–238, Aug. 2016.

[8] T. Kruhn, S. Falkenberg, and L. Overmeyer, "Decentralized control for small-scaled conveyor modules with cellular automata," in *Proc. IEEE Int. Conf. Autom. Logistics*, Aug. 2010, pp. 237–242.

[9] T. Kruhn, M. Radosavac, N. Shchekutin, and L. Overmeyer, "Decentralized and dynamic routing for a cognitive conveyor," in *Proc. IEEE/ASME Int. Conf. Adv. Intell. Mechatronics*, Jul. 2013, pp. 436–441.

[10] Z. Seibold, T. Stoll, and K. Furmans, "Layout-optimized sorting of goods with decentralized controlled conveying modules," in *Proc. IEEE Int. Syst. Conf. (SysCon)*, Apr. 2013, pp. 628–633.

[11] T. Kruhn, S. Sohrt, and L. Overmeyer, "Mechanical feasibility and decentralized control algorithms of small-scale, multi-directional transport modules," *Logistics Res.*, vol. 9, no. 1, pp. 1–14, Dec. 2016.

[12] T. Sun, Y. Zhang, H. Zhang, P. Wang, Y. Zhao, and G. Liu, "Three-wheel driven omnidirectional reconfigurable conveyor belt design," in *Proc. Chin. Autom. Congr. (CAC)*, Nov. 2019, pp. 101–105.

[13] C. Uriarte, A. Asphandiar, H. Thamer, A. Benggolo, and M. Freitag, "Control strategies for small-scaled conveyor modules enabling highly flexible material flow systems," *Proc. CIRP*, vol. 79, pp. 433–438, Jan. 2019.

[14] J. S. Keek, S. L. Loh, and S. H. Chong, "Design and control system setup of an E-pattern omniwheeled cellular conveyor," *Machines*, vol. 9, no. 2, p. 43, Feb. 2021.

[15] W. Zaher, A. W. Youssef, L. A. Shihata, E. Azab, and M. Mashaly, "Omnidirectional-wheel conveyor path planning and sorting using reinforcement learning algorithms," *IEEE Access*, vol. 10, pp. 27945–27959, 2022.

[16] M. R. Azizi, A. Rastegarpanah, and R. Stolkin, "Motion planning and control of an omnidirectional mobile robot in dynamic environments," *Robotics*, vol. 10, no. 1, p. 48, Mar. 2021.

[17] C. Ren, Y. Ding, X. Li, X. Zhu, and S. Ma, "Extended state observer based robust friction compensation for tracking control of an omnidirectional mobile robot," *J. Dyn. Syst., Meas., Control*, vol. 141, no. 10, May 2019.

[18] J. Palacín, E. Rubies, E. Clotet, and D. Martínez, "Evaluation of the path-tracking accuracy of a three-wheeled omnidirectional mobile robot designed as a personal assistant," *Sensors*, vol. 21, no. 21, p. 7216, Oct. 2021.

[19] S. Jeong and D. Chwa, "Sliding-mode-disturbance-observer-based robust tracking control for omnidirectional mobile robots with kinematic and dynamic uncertainties," *IEEE/ASME Trans. Mechatronics*, vol. 26, no. 2, pp. 741–752, Apr. 2021.

[20] H.-M. Wu and M. Karkoub, "Frictional forces and torques compensation based cascaded sliding-mode tracking control for an uncertain omnidirectional mobile robot," *Meas. Control*, vol. 55, nos. 3–4, pp. 178–188, Mar. 2022.

[21] L. Ovalle, H. Ríos, M. Llama, V. Santibáñez, and A. Dzul, "Omnidirectional mobile robot robust tracking: Sliding-mode output-based control approaches," *Control Eng. Pract.*, vol. 85, pp. 50–58, Apr. 2019.

[22] R. Singh and T. K. Bera, "Fuzzy logic controller for obstacle avoidance of mobile robot," *Int. J. Nonlinear Sci. Numer. Simul.*, vol. 20, no. 1, pp. 51–62, Feb. 2019, doi: 10.1515/ijnsns-2018-0038.

[23] H. Xue, Z. Zhang, M. Wu, and P. Chen, "Fuzzy controller for autonomous vehicle based on rough sets," *IEEE Access*, vol. 7, pp. 147350–147361, 2019.

[24] K. Akka and F. Khaber, "Optimal fuzzy tracking control with obstacles avoidance for a mobile robot based on Takagi–Sugeno fuzzy model," *Trans. Inst. Meas. Control*, vol. 41, no. 10, pp. 2772–2781, Jun. 2019.

[25] C. Zong, Z. Ji, Y. Yu, and H. Shi, "Research on obstacle avoidance method for mobile robot based on multisensor information fusion," *Sensors Mater.*, vol. 32, no. 4, pp. 1159–1170, 2020.

[26] J. Lv, C. Qu, S. Du, X. Zhao, P. Yin, N. Zhao, and S. Qu, "Research on obstacle avoidance algorithm for unmanned ground vehicle based on multi-sensor information fusion," *Math. Biosci. Eng.*, vol. 18, no. 2, pp. 1022–1039, 2021.

[27] H.-T. Yau and C.-L. Chen, "Chattering-free fuzzy sliding-mode control strategy for uncertain chaotic systems," *Chaos, Solitons Fractals*, vol. 30, no. 3, pp. 709–718, Nov. 2006.

[28] S. J. Chapman, *Fortran 90/95 for Scientists and Engineers*, 1st ed. New York, NY, USA: McGraw-Hill, 1998.
[29] *MATLAB The Language of Technical Computing: Function Reference*, The MathWorks, Natick, MA, USA, 2004.
[30] V. Torres and J. Valls, "A fast and low-complexity operator for the computation of the arctangent of a complex number," *IEEE Trans. Very Large Scale Integr. (VLSI) Syst.*, vol. 25, no. 9, pp. 2663–2667, Sep. 2017.
[31] V. Torres, J. Valls, and R. Lyons, "Fast- and low-complexity atan2(a,b) approximation [tips and tricks]," *IEEE Signal Process. Mag.*, vol. 34, no. 6, pp. 164–169, Nov. 2017.

MUHAMMAD QOMARUZ ZAMAN received the bachelor's and master's degrees in electrical engineering from Institut Teknologi Sepuluh Nopember, Surabaya, Indonesia, in 2018. He is currently pursuing the Ph.D. degree with the National Taipei University of Technology. From 2015 to 2018, he was a Research Assistant with the Microcontroller Laboratory, Institut Teknologi Sepuluh Nopember. His research interests include robotics and the IoT.

HSIU-MING WU (Senior Member, IEEE) received the Ph.D. degree from the Department of Electrical Engineering, National Taiwan University of Science and Technology, in 2009. He was a Postdoctoral Fellow with the Opto-Mechatronics Technology Center, National Taiwan University of Science and Technology. In early 2013, he was a Postdoctoral Fellow with Texas A&M University, Qatar, for four years. In early 2018, he joined the Department of Mechanical Engineering, National Chin-Yi University of Technology, Taichung, for two years. Currently, he is an Assistant Professor with the Department of Intelligent Automation Engineering, National Taipei University of Technology. His research interests include mechatronics, nonlinear control, and robotic control.